Available online at www.sciencedirect.com

ScienceDirect

Solar Energy 115 (2015) 33–39

SOLAR ENERGY

www.elsevier.com/locate/solener

Ab initio method of optical investigations of $CdS_{1-x}Te_x$ alloys under quantum dots diameter effect

Y. Al-Douri [a,b,*], U. Hashim [a], R. Khenata [c,d], A.H. Reshak [e,f], M. Ameri [g], A. Bouhemadou [h], A. Rahim Ruslinda [a], M.K. Md Arshad [a]

[a] Institute of Nano Electronic Engineering, University Malaysia Perlis, 01000 Kangar, Perlis, Malaysia
[b] Physics Department, Faculty of Science, University of Sidi-Bel-Abbes, 22000, Algeria
[c] Laboratoire de Physique Quantique et de Modélisation Mathématique (LPQ3M), Université de Mascara, 29000 Mascara, Algeria
[d] Department of Physics and Astronomy, Faculty of Science, King Saud University, P.O. Box 2455, Riyadh 11451, Saudi Arabia
[e] New Technologies – Research Centre, University of West Bohemia, Univerzitni 8, 306 14 Pilsen, Czech Republic
[f] Center of Excellence Geopolymer and Green Technology, School of Material Engineering, University Malaysia Perlis, 01007 Kangar, Perlis, Malaysia
[g] Department of Physics, University of Djillali Liabes, Sidi Bel-Abbes 22000, Algeria
[h] Laboratory for Developing New Materials and their Characterization, Department of Physics, Faculty of Science, University of Setif, 19000 Setif, Algeria

Received 11 November 2014; received in revised form 5 February 2015; accepted 19 February 2015

Communicated by: Associate Editor Takhir M. Razykov

Abstract

The indirect energy gap ($\Gamma-X$) is calculated using density functional theory (DFT) of the full potential-linearized augmented plane wave (FP-LAPW) method as implemented in WIEN2K code. The Engel–Vosko generalized gradient approximation (EV-GGA) formalism is used to optimize the corresponding potential for energetic transition and optical properties calculations of $CdS_{1-x}Te_x$ alloys as a function of quantum dot diameter and is used to test the validity of our model of quantum dot potential. The refractive index and optical dielectric constant are investigated to explore best applications for solar cells.

Keywords: Quantum dot potential; Alloys; Optical properties

1. Introduction

The main feature of each solar cell is its capability to absorb effectively wide spectrum of photons contained in solar radiation reaching its active surface. This feature depends on intrinsic optical and electronic properties of semiconductor material, and the critical parameter related to semiconductor is energy band gap and energy band structure. Among available thin-film solar cell (α-Si, $CuInGaSe_2$ and CdTe) materials, cadmium telluride (CdTe) may be the strongest candidate for high throughput, large-scale manufacturing (Hsu et al., 2012) of polycrystalline thin-film solar cells. Because of its high absorption coefficient ($>1\times10^4\,cm^{-1}$) and direct band-gap (1.5 eV), about 1 μm thick CdTe film is enough for absorption of ~90% of photons with energy higher than its band gap. However, the availability of elemental Te may be a concern if production levels increase above 20 GW per year (Boucher et al., 2014). It is advantageous to use the computational method based on total energy calculations to study the phase transition from the

* Corresponding author at: Institute of Nano Electronic Engineering, University Malaysia Perlis, 01000 Kangar, Perlis, Malaysia. Tel.: +60 49775021; fax: +60 49798578.
E-mail address: yaldouri@yahoo.com (Y. Al-Douri).

http://dx.doi.org/10.1016/j.solener.2015.02.024
0038-092X/

coordinated number Nc = 4 to 6-fold (Zhang and Cohen, 1987). Third-generation approaches to photovoltaics (PVs) aim to decrease costs and significantly increasing efficiencies but maintaining the economic and environmental cost advantages of thin-film deposition techniques (Green, 2003). There are several approaches to achieve such multiple energy threshold devices (Green, 2003; Nelson, 2003); tandem or multicolor cells, concentrator systems, intermediate-level cells, multiple carrier excitation, up/down conversion and hot carrier cells (Conibeer, 2007).

Recently, Yum et al. (2014) have demonstrated PbS:Hg quantum dots-sensitized solar cell (QDSC) combined with a dye-sensitized solar cell (DSC) to harvest panchromatic solar spectrum from the visible light to the near IR. They have used the filter to split the solar energy and access the total conversion efficiency. The DSC performing 12.4% under AM1.5G sunlight was able to generate 9.1% with a short-wave pass filter cutting off photons of wavelength longer than 650 nm. On the other hand, QDSC performing 5.58% generated 3.42% with the use of a long-wave pass filter transmitting beyond 630 nm. Calculated based on transmitted light, DSC and QDSC performed 24.0% and 5.90%, leading to almost 13.1% of estimated total power conversion efficiency by harvesting the solar energy from visible light to the NIR. While, Badawi et al. (2013) have studied the photovoltaic performance of CdTe quantum dots (QDs) sensitized solar cells (QDSSCs) as a function of tuning the band gap of CdTe QDs size. Presynthesized CdTe QDs of radii from 2.1 nm to 2.5 nm were deposited by direct adsorption (DA) technique onto a layer of TiO_2 nanoparticles (NPs) to serve as sensitizers for the solar cells. The characteristic parameters of the assembled QDSSCs were measured under AM 1.5 sun illuminations. The values of current density (J_{sc}) and overall efficiency (η) increase with decreasing CdTe QDs size, since the lowest unoccupied molecular orbital (LUMO) levels shifts closer to vacuum level, which causes an increase in the driving force. Furthermore, the photocurrent response of the assembled cells to ON OFF cycles of the illumination indicates the prompt generation of anodic current. Moreover, Emin et al. (2011) have reviewed the recent progresses in various quantum dot solar cells that are prepared from colloidal quantum dots. They have discussed the preparation methods, working concepts, advantages and disadvantages of different device architectures. Major topics include integration of colloidal quantum dots in: Schottky solar cells, depleted heterojunction solar cells, extremely thin absorber solar cells, hybrid organic–inorganic solar cells, bulk heterojunction solar cells and quantum dot sensitized solar cells. However, Udipi et al. (1996) have presented semiclassical simulation results for the potential energy profile and electron density distribution in 200 nm silicon quantum dot. For the solution of the continuity equation, the efficient difference approximations, proposed by Scharfetter and Gummel (1969) extended to three dimensions. In essence, they have followed the two-dimensional approach due to Selberherr et al. (1980) extend two to three dimensions.

The investigation of further materials research is interesting when one tries to gain some information about the diameter dependence of the compounds; especially it is proved with some of the materials (Al-Douri et al., 2011; 2012). It seems more fundamental to relate the diameter dependence behavior to the bonds between nearest atoms. By controlling the evolution with diameter dependence of the compound, it could attempt to link the effect of quantum dot diameter to the quantum dot potential. In this context, we have used this procedure for testing the validity of our model (Al-Douri, 2009) of QDs potential. The obtained energy band gaps are used to calculate the quantum dot potential and to predict materials for QD's. The aim of this paper is to verify our model (Al-Douri, 2009) for calculating the diameter dependence on QDs potential for dot diameters down to 57 nm, 58 nm and 60 nm for $CdS_{0.75}Te_{0.25}$, $CdS_{0.5}Te_{0.5}$ and $CdS_{0.25}Te_{0.75}$ alloys, respectively using the full potential linearized augmented plane wave (FP-LAPW), in addition to investigate the optical properties of refractive index and optical dielectric constant using specific models for the mentioned alloys.

2. Calculations

The effect of tellurium concentration on the optical properties of the cadmium sulfide telluride $CdS_{1-x}Te_x$ ternary alloys ($x = 0.0, 0.25, 0.5, 0.75, 1.0$) is studied using the full potential linearized augmented plane wave method. Recently, the 'special quasirandom structures' (SQS) Zunger's approach (Zunger et al., 1990) is used to reproduce the randomness of the alloys for the first few shells around a given site. The alloys for many physical properties that are not affected by the errors introduced by using the concept of the periodicity beyond the first few shells are described using this approach which is reasonably sufficient.

The calculations were carried out using the full potential linearized augmented plane wave (FP-LAPW) method as implemented in WIEN2 K code (Blaha et al., 2001). The exchange correlation potential was treated using the generalized gradient approximation (GGA) Perdew et al., 1996 for the total energy calculations and the Engel–Vosko GGA (EVGGA) formalism Engel and Vosko, 1993 for principal energy calculations. To overcome the shortcoming of both LDA and GGA of underestimation the energy gap (Dufek et al., 1994) we have used EVGGA. This shortcoming is ascribed to the fact that they do not reproduce the exchange correlation energy and its charge derivative correctly. Hence, the modified form of GGA is the EVGGA, which is capable to better reproduce the exchange potential at the expense of less agreement in the exchange energy, which yields a better band splitting. The calculations of quantities that depend on an accurate description of the exchange potential as the equilibrium volume and bulk modulus using EVGGA are in poor

agreement with experiment (Dufek et al., 1994). In the FP-LAPW method, the wave function, charge density and potential were expanded by spherical harmonic functions inside non-overlapping spheres surrounding the atomic sites (muffin-tin spheres) and by plane waves basis set in the remaining space of the unit cell (interstitial region). The maximal l value for the wave function expansion inside the atomic spheres was confined to $l_{max} = 10$. The muffin-tin radii were assumed to be 1.6 atomic units (a.u.) for S, and 1.95 for both Cd and Te. The plane wave cut-off of $K_{max} = 9.0/RMT$ was chosen for the expansion of the wave functions in the interstitial region for the parent CdS, CdTe binary compounds and $CdS_{1-x}Te_x$ ternary alloy while the charge density is Fourier expanded up to $G_{max} = 14$ $(Ryd)^{1/2}$. The irreducible wedge of the Brillouin zone was described by a mesh of 35 special k-points for binary compounds and alloys except for the case of $x = 0.5$, where we used a mesh of 64 special k-points. In the case of principal energy calculations, we used denser meshes of 220 k-points for binary as well as ternary alloys of $x = 0.25$ and 0.75, whereas 216 k-points were used for $x = 0.5$. The self-consistent calculations are converged since the total energy of the system is stable within 10^{-5} Ry.

3. Results and discussion

The covalent semiconductors are four-fold coordinated. The reason that the density of structure is so low and the nearest neighbors of atoms are bound by overlapping hybridized orbitals, which are the well-known sp^3 hybrids with tetrahedral shape. Hence, it is possible to tune the energy band gaps using dot diameter. The calculated values of the direct ($\Gamma \rightarrow \Gamma$) and the indirect ($\Gamma \rightarrow X$) and ($\Gamma \rightarrow L$) energy band gaps within EVGGA of the investigated $CdS_{1-x}Te_x$ alloys at different dot diameters are listed in Table 1 along with the experimental data (Lincot and Hodes, 2006; Tsidilkovski, 1982) and other theoretical calculations (Feng et al., 1993; Al-Douri et al., 2001). Our calculated values of the ($\Gamma \rightarrow \Gamma$) energy band gap is slightly underestimated compared to the experimental data. This could be attributed to our use of the EVGGA approximation. Due to these values, $CdS_{1-x}Te_x$ alloys have been classified as direct energy band gap semiconductor. Because of their use in infrared light generation and detection, the energy gap variations of dot diameters represent an important property to study. As mentioned at Table 1, the energy band gaps correlate inversely with the dot diameters and confirmed by Fig. 1.

The energy band gaps between the valence band maximum (VBM) at the point Γ and the conduction band minimum (CBM) at the point X are computed based on the FP-LAPW. By means of our recent model (Al-Douri, 2009), the quantum dot potential has evaluated, according to the formula:

$$\boldsymbol{P}_{QD} = \frac{b}{a} \cdot \boldsymbol{E}_{g\Gamma X} \cdot 10^{-3} \cdot \lambda \qquad (1)$$

Table 1
The calculated principal energy gaps for $CdS_{0.75}Te_{0.25}$, $CdS_{0.5}Te_{0.5}$ and $CdS_{0.25}Te_{0.75}$ alloys (in eV) at different QD's diameters (in nm) compared to other experimental data and theoretical results.

QD's diameter	E_g (Γ–Γ)	E_g (Γ–X)	E_g (Γ–L)
CdS	2.359, 2.42[a] 2.361[b]	4.626	3.432
CdTe	1.368 1.8[c] 1.8[d]	3.241	2.288
$CdS_{0.75}Te_{0.25}$			
61	0.943	0.943	2.484
60	1.067	0.949	2.609
59	1.187	0.955	2.731
58.5	1.306	0.960	2.850
58	1.422	0.964	2.967
57.5	1.535	0.968	3.082
$CdS_{0.5}Te_{0.5}$			
63	0.730	2.737	2.583
61.5	0.853	2.743	2.707
60.5	0.974	2.748	2.829
60	1.092	2.753	2.949
59	1.208	2.758	3.066
58	1.321	2.761	3.180
$CdS_{0.25}Te_{0.75}$			
65	0.650	0.650	1.538
63.5	0.774	0.657	1.663
62.5	0.895	0.662	1.785
61.5	1.013	0.667	1.940
61	1.129	0.670	2.021
60	1.242	0.675	2.136

[a] Reference Lincot and Hodes (2006) Expt.
[b] Reference Feng et al. (1993) Theor.
[c] Reference Tsidilkovski (1982) Expt.
[d] Reference Al-Douri et al. (2001) Theor.

where $\frac{b}{a}$ is constant (in eV^{-1}) [see Table 4 in Al-Douri {2009), $\boldsymbol{E}_{g\Gamma X}$ is the energy gap along $\Gamma - X$ (in eV) and λ is an appropriate parameter for group-IV ($\lambda = 6$), III–V ($\lambda = 4$) and II–VI ($\lambda = 2$) semiconductors (in V).

A correlation between QDs diameter and pressure effect changes is stated. If quantum dot diameter is changed, the strong sp^3 covalent bonding that characterizes the covalent structure is affected. From our viewpoint, this discrepancy at diameter dependence is an immediate consequence of the difference in the corresponding quantum dot potential. In Table 2, the calculated quantum dot potential at quantum diameter dependence is computed.

The critical dot diameter is the value that separates the decrease and the increase of the QDs potential. The diameter dependence correlates with transition pressure (P_t) that is important to be computed from difference in molar free energies of compounds. The Gibbs free-energy difference, ΔG_t, between compounds which has the tetrahedral coordination at diameter dependence is nearly given by $\Delta G = \Delta H - T\Delta S$ (in kJ mol^{-1}) where H is enthalpy, T is temperature and S is entropy. Most of energies are larger for smaller bond lengths. Changing the QDs potential with dot diameter is confirmed by the change of the energy gaps at principal points (Γ–Γ, Γ–X and Γ–L) as shown in

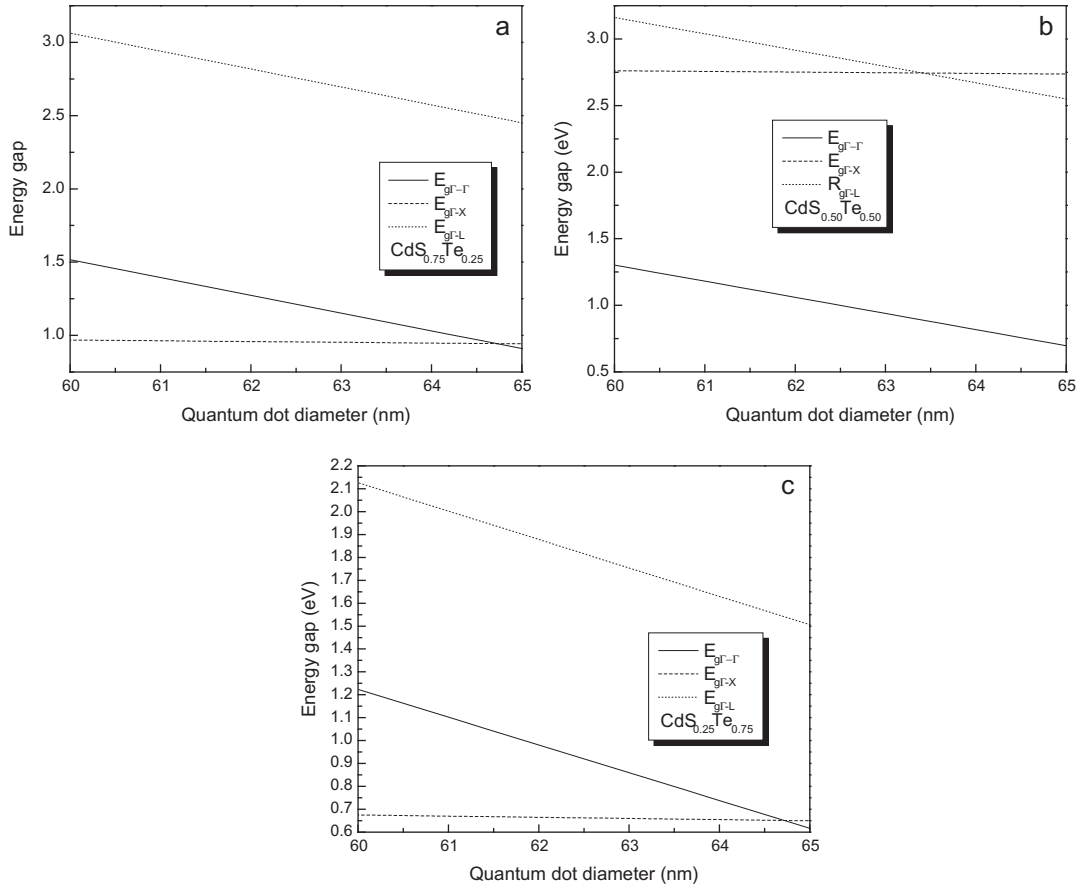

Fig. 1. Calculated energy band gaps direct ($\Gamma \rightarrow \Gamma$), and indirect ($\Gamma \rightarrow X$) and ($\Gamma \rightarrow L$) for (a) $CdS_{0.75}Te_{0.25}$, (b) $CdS_{0.5}Te_{0.5}$ and (c) $CdS_{0.25}Te_{0.75}$ alloys as a function of QDs diameter.

Table 2
The calculated quantum dot potential for $CdS_{0.75}Te_{0.25}$, $CdS_{0.5}Te_{0.5}$ and $CdS_{0.25}Te_{0.75}$ alloys (in mV) compared to other value at different QD's diameters (in nm).

QD's diameter	P_{QD} cal.	P_{QD} (Udipi et al., 1996)
$CdS_{0.75}Te_{0.25}$		
61	0.1793	$\leqslant 1$
60	0.1804	
59	0.1815	
58.5	0.1825	
58	0.1833	
57.5	0.1840	
$CdS_{0.5}Te_{0.5}$		
63	0.5200	$\leqslant 1$
61.5	0.5212	
60.5	0.5222	
60	0.5232	
59	0.5240	
58	0.5247	
$CdS_{0.25}Te_{0.75}$		
65	0.1236	$\leqslant 1$
63.5	0.1248	
62.5	0.1259	
61.5	0.1268	
61	0.1276	
60	0.1284	

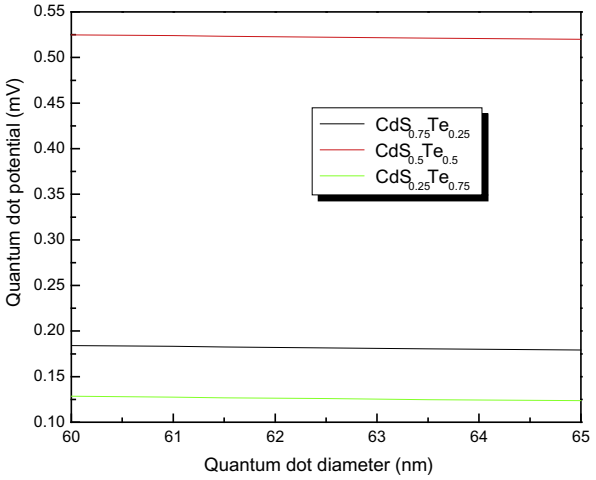

Fig. 2. QDs diameter dependence of the quantum dot potential for $CdS_{0.75}Te_{0.25}$, $CdS_{0.5}Te_{0.5}$ and $CdS_{0.25}Te_{0.75}$ alloys.

Table 1. The QDs potential varies inversely with quantum diameter (Table 2) and confirmed by Fig. 2. The relationship is almost linear for $CdS_{1-x}Te_x$ alloys. Consequently, fluctuations of the QDs potential appear. Our calculated QDs potential values are in accordance with other data

(Udipi et al., 1996). It is mentioned that the variation of the QDs potential is an indication of the electron tunnels the quantum dot.

The refractive index n is a very important physical parameter related to the microscopic atomic interactions. From theoretical viewpoint, there are two different approaches of viewing this subject: firstly; the refractive index will be related to the density and local polarizability and secondly; the refractive index will be closely related to the energy band structure of the material, through the dielectric constant. (Balzaretti and da Jornada, 1996). Consequently, many attempts have been made in order to relate the refractive index and the energy gap E_g through simple relationships (Moss, 1950; Gupta and Ravindra, 1980; Al-Douri et al., 2008, 2010; Herve and Vandamme, 1993; Ravindra et al., 1979). However, these relations of n are independent of temperature and incident photon energy. Here the various relations between n and E_g will be reviewed. Ravindra et al. (1979) had presented a linear form of n as a function of E_g:

$$n = \alpha + \beta E_g \tag{2}$$

where $\alpha = 4.048$ and $\beta = -0.62\,\mathrm{eV}^{-1}$. (Herve and Vandamme, 1995) have proposed an empirical relation as follows:

$$n = \sqrt{1 + \left(\frac{A}{E_g + B}\right)^2} \tag{3}$$

where $A = 13.6$ eV and $B = 3.4$ eV. For group II–IV semiconductors, Ghosh et al. (1984) have published an empirical relationship based on the band structure and quantum dielectric considerations of Penn (1962) and (Van Vechten, 1969):

$$n^2 - 1 = \frac{A}{(E_g + B)^2} \tag{4}$$

where $A = 8.2E_g + 134$, $B = 0.225E_g + 2.25$ and $(E_g + B)$ refers to an appropriate average energy gap of the material. Thus, using these three models the variation of n with dot diameter has been calculated. The results are displayed in Fig. 3. The calculated refractive indices and the optical dielectric constants of the end-point compounds are investigated and listed in Table 3.

This is verified by the calculation of the optical dielectric constant ε_∞, which depends on the refractive index. Note that $\varepsilon_\infty = n^2$ (Samara, 1983). It is clear that the calculated n using the model of Herve and Vandamme (1995) is an appropriate one due to reflectivity parameter is important in enhancing the photo conversion for solar cells. Again,

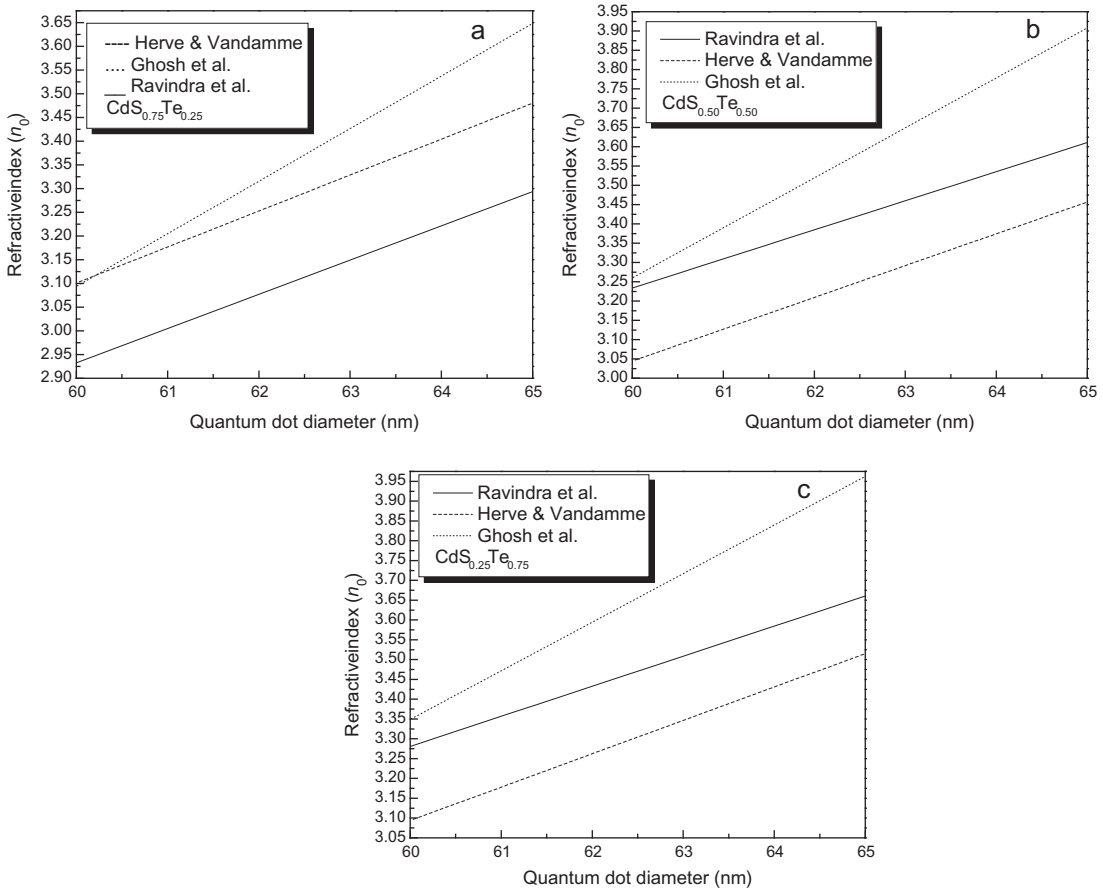

Fig. 3. QDs diameter dependence of the refractive index (n) for (a) $CdS_{0.75}Te_{0.25}$ (b) $CdS_{0.5}Te_{0.5}$ and (c) $CdS_{0.25}Te_{0.75}$ alloys.

Table 3
Calculated refractive indices for $CdS_{0.75}Te_{0.25}$, $CdS_{0.5}Te_{0.5}$ and $CdS_{0.25}Te_{0.75}$ alloys at diameter dependence using Ravindra et al. (1979), Herve and Vandamme (1995) and Ghosh et al. (1984) models corresponding to optical dielectric constant.

QD's diameter	n	ε_∞
CdS	2.589[a] 2.567[b] 2.611[c] 2.38[*]	6.702[a] 2.589[b] 2.817[c]
CdTe	3.345[a] 3.1627[b] 3.439[c] 2.7[*]	11.189[a] 9.998[b] 11.826[c]
$CdS_{0.75}Te_{0.25}$		
61	3.46[a] 3.28[b] 3.63[c]	11.97[a] 10.75[b] 13.17[c]
60	3.38[a] 3.20[b] 3.50[c]	11.42[a] 10.24[b] 12.25[c]
59	3.31[a] 3.12[b] 3.38[c]	10.95[a] 9.73[b] 11.42[c]
58.5	3.23[a] 3.05[b] 3.28[c]	10.43[a] 9.30[b] 10.75[c]
58	3.16[a] 2.99[b] 3.18[c]	9.98[a] 8.94[b] 10.11[c]
57.5	3.09[a] 2.93[b] 3.09[c]	9.54[a] 8.58[b] 9.54[c]
$CdS_{0.5}Te_{0.5}$		
63	3.59[a] 3.44[b] 3.89[c]	12.88[a] 11.83[b] 15.13[c]
61.5	3.51[a] 3.35[b] 3.73[c]	12.32[a] 11.22[b] 13.91[c]
60.5	3.44[a] 3.26[b] 3.60[c]	11.83[a] 10.62[b] 12.96[c]
60	3.37[a] 3.18[b] 3.47[c]	11.35[a] 10.11[b] 12.04[c]
59	3.29[a] 3.11[b] 3.36[c]	10.82[a] 9.67[b] 11.28[c]
58	3.22[a] 3.04[b] 3.26[c]	10.36[a] 9.24[b] 10.62[c]
$CdS_{0.25}Te_{0.75}$		
65	3.64[a] 3.50[b] 3.91[c]	13.24[a] 12.25[b] 15.28[c]
63.5	3.56[a] 3.40[b] 3.83[c]	12.67[a] 11.56[b] 14.66[c]
62.5	3.49[a] 3.32[b] 3.69[c]	12.18[a] 11.02[b] 13.61[c]
61.5	3.41[a] 3.23[b] 3.55[c]	11.62[a] 10.43[b] 12.60[c]
61	3.34[a] 3.16[b] 3.44[c]	11.15[a] 9.98[b] 11.83[c]
60	3.27[a] 3.09[b] 3.33[c]	10.69[a] 9.54[b] 11.08[c]

[a] Reference Ravindra et al. (1979).
[b] Reference Herve and Vandamme, (1995).
[c] Reference Ghosh et al., (1984).
[*] Reference Ravindra et al., (1979) Expt.

a linear dependence of the $CdS_{1-x}Te_x$ alloys properties on the dot diameter is observed and that the refractive index for small diameter dependence tends to shift toward the blue–green. It means a high absorption and low reflection spectrum may be attributed to increase solar cells efficiency. This work regards an impetus for researching further materials for both theoreticians and experimentalists to improve the solar energy applications.

4. Conclusion

The FP-LAPW method provides a good way to calculate the electronic properties and investigate optical properties of low reflectivity value for $CdS_{1-x}Te_x$ alloys and prove that 57 nm, 58 nm and 60 nm for $CdS_{0.75}Te_{0.25}$, $CdS_{0.5}Te_{0.5}$ and $CdS_{0.25}Te_{0.75}$ alloys, respectively using Herve and Vandamme are more suitable for solar cells applications, expecting new trends for other alloys and new realization for quantum dots.

Acknowledgments

This work has been achieved using FRGS grants numbered: 9007-00111. One of us; Y. A. would like to acknowledge TWAS-Italy, for full support of his visit to JUST-Jordan under TWAS-UNESCO Associateship.

The author A.H.R. would like to acknowledge the CENTEM project, reg. no. CZ.1.05/2.1.00/03.0088, cofunded by the ERDF as part of the Ministry of Education, Youth and Sports OP RDI programme and, in the follow-up sustainability stage, supported through CENTEM PLUS (LO1402) by financial means from the Ministry of Education, Youth and Sports under the "National Sustainability Programme I". Computational resources were provided by MetaCentrum (LM2010005) and CERIT-SC (CZ.1.05/3.2.00/08.0144) infrastructures.

References

Al-Douri, Y., 2009. Quantum dot modeling of semiconductors. In: Reshak, Ali H. (Ed.), Advances in Condensed Matter Physics. Research Signpost, Kerala, India, pp. 55–70.
Al-Douri, Y., Abid, H., Zaoui, A., Aourag, H., 2001. Correlation between the iconicity character and the heteropolar energy band gap in semiconductors. Physica B 301, 295–298.
Al-Douri, Y., Feng, Y.P., Huan, A.C.H., 2008. Optical investigations using ultra-soft pseudopotential calculations of $Si_{0.5}Ge_{0.5}$ alloy. Solid State Commun. 148, 521–524.
Al-Douri, Y., Reshak, A.H., Baaziz, H., Charifi, Z., Khenata, R., Ahmad, S., Hashim, U., 2010. An ab initio study of the electronic structure and optical properties of $CdS_{1-x}Te_x$ alloys. Solar Energy 84, 1979–1984.
Al-Douri, Y., Khenata, R., Reshak, A.H., 2011. Investigated optical studies of Si quantum dot. Solar Energy 85, 2283–2287.
Al-Douri, Y., Baaziz, H., Charifi, Z., Khenata, R., Hashim, U., Al-Jassim, M., 2012. Further optical properties of CdX (X = S, Te) compounds under quantum dot diameter effect: ab initio method. Renew. Energy 45, 232–236.
Badawi, A., Al-Hosiny, N., Abdallah, S., Negm, S., Talaat, H., 2013. Tuning photocurrent response through size control of CdTe quantum dots sensitized solar cells. Solar Energy 88, 137–143.
Balzaretti, N.M., da Jornada, J.A.H., 1996. Pressure dependence of the refractive index of diamond, cubic silicon carbide and cubic boron nitride. Solid State Commun. 99, 943–948.
Blaha, P., Schwarz, K., Madsen, G.K.H., Kvasnicka, D., Luitz, J. WIEN2K, Techn. Universitat, Wien, Austria, ISBN 3-9501031-1-1-2 (2001).
Boucher, J.W., Miller, D.W., Warren, C.W., Cohen, J.D., McCandless, B.E., Heath, J.T., Lonergan, M.C., Boettcher, S.W., 2014. Optical response of deep defects as revealed by transient photocapacitance and photocurrent spectroscopy in CdTe/CdS solar cells. Solar Energy Mater. Solar Cells 129, 57–63.
Conibeer, G., 2007. Third-generation photovoltaics. Mater. Today 10, 42–50.
Dufek, P., Blaha, P., Schwarz, K., 1994. Applications of Engel and Vosko's generalized gradient approximation in solids. Phys. Rev. B 50, 7279–7292.
Emin, S., Singh, S.P., Han, L., Satoh, N., Islam, A., 2011. Colloidal quantum dot solar cells. Solar Energy 85, 1264–1282.
Engel, E., Vosko, S.H., 1993. Exact exchange-only potentials and the virial relation as microscopic criteria for generalized gradient approximations. Phys. Rev. B 47, 13164–13175.
Feng, Y.P., Teo, K.L., Li, M.F., Poon, H.C., Ong, C.K., Xia, J.B., 1993. Empirical pseudopotential band-structure calculation for $Zn_{1-x}Cd_xS_ySe_{1-y}$ quaternary alloy. J. Appl. Phys. 74, 3948–3955.
Ghosh, D.K., Samanta, L.K., Bhar, G.C., 1984. A simple model for evaluation of refractive index of some binary and ternary mixed crystals. Infrared Phys. 24, 43–47.
Green, M.A., 2003. Third Generation Photovoltaics: Ultra-High Efficiency at Low Cost. Springer-Verlag, Berlin, pp. 110–135.

Gupta, V.P., Ravindra, N.M., 1980. Comments on the Moss Formula. Phys. Stat. Sol. (b) 100, 715–719.
Herve, P., Vandamme, L.K.J., 1993. General relation between refractive index and energy gap in semiconductors. Infrared Phys. Technol. 35, 609–615.
Herve, P.J.L., Vandamme, L.K.J., 1995. Empirical temperature dependence of the refractive index of semiconductors. J. Appl. Phys. 77, 5476–5477.
Hsu, H.-R., Hsu, S.-C., Liu, Y.S., 2012. Improvement of Ga distribution and enhancement of grain growth of $CuInGaSe_2$ by incorporating a thin CuGa layer on the single CuInGa precursor. Solar Energy 86, 48–52.
Lincot, D., Hodes, G., 2006. Chemical Solution Deposition of Semiconducting and Non-Metallic Films. Electrochemical Society, USA, pp. 1–13.
Moss, T.S., 1950. A relationship between the refractive index and the infra-red threshold of sensitivity for photoconductors. Proc. Phys. Soc. B. 63, 167–173.
Nelson, J., 2003. The Physics of Solar Cells. Imperial College Press, London, pp. 175–215.
Penn, D.R., 1962. Wave-number-dependent dielectric function of semiconductors. Phys. Rev. 128, 2093–2097.
Perdew, J.P., Burke, S., Ernzerhof, M., 1996. Generalized gradient approximation made simple. Phys. Rev. Lett. 77, 3865–3869.
Ravindra, N.M., Auluck, S., Srivastava, V.K., 1979. On the Penn Gap in Semiconductors. Phys. Stat. Sol. (b) 93, K155–K160.
Samara, G.A., 1983. Temperature and pressure dependences of the dielectric constants of semiconductors. Phys. Rev. B 27, 3494–3505.
Scharfetter, D.L., Gummel, H.K., 1969. Large-signal analysis of a silicon read diode oscillator. IEEE Trans. Electron. Dev. 16, 64–77.
Selberherr, S., Shutz, A., Potzl, H.W., 1980. MINIMOS—A two-dimensional MOS transistor analyzer. IEEE Trans. Electron. Dev. 27, 1540–1550.
Tsidilkovski, I.M., 1982. Band Structure of Semiconductors. Pergamon Press, Oxford, pp. 102–105.
Udipi, S., Vasileska, D., Ferry, D.K., 1996. Numerical modeling of silicon quantum dots. Superlattices Microstruct. 20, 343–347.
Van Vechten, J.A., 1969. Quantum dielectric theory of electronegativity in covalent systems. I. Electronic dielectric constant. Phys. Rev. 182, 891–905.
Yum, J.-H., Lee, J.-W., Kim, Y., Humphry-Baker, R., Park, N.-G., Grätzel, M., 2014. Panchromatic light harvesting by dye- and quantum dot-sensitized solar cells. Solar Energy 109, 183–188.
Zhang, S.B., Cohen, M.L., 1987. High-pressure phases of III–V zinc-blende semiconductors. Phys. Rev. B 35, 7604–7610.
Zunger, A., Wei, S.-H., Ferreira, L.G., Bernard, E., 1990. Special quasirandom structures. Phys. Rev. Lett. 65, 353–358.